Available online at www.sciencedirect.com
ScienceDirect
Dyes and Pigments 75 (2007) 619–623
DYES and PIGMENTS
www.elsevier.com/locate/dyepig

Novel bent-shaped liquid crystalline compounds: III. Synthesis of Schiff base liquid crystal dimers

Bong-Keun So [a], Wha-Jong Kim [a], Soo-Min Lee [a,*], Min-Cheol Jang [b], Hyun Hoon Song [b], Joo-Hoon Park [c]

[a] *Department of Chemistry, Hannam University, Taejon 306-791, Republic of Korea*
[b] *Department of Polymer Science and Engineering, Hannam University, Taejon 306-791, Republic of Korea*
[c] *School of Natural Science, Hoseo University, Choongnam 336-795, Republic of Korea*

Received 3 July 2006; received in revised form 6 July 2006; accepted 6 July 2006
Available online 6 September 2006

Abstract

A group of new bent-shaped mesomorphic compounds with two identical mesogens (Schiff base), which have 2-hydroxy-1,3-dioxypropylene ($-OCH_2CH(OH)CH_2O-$) as a short spacer unit, and different lengths of terminal alkoxy chains ($-OC_nH_{2n+1}$; $n = 5-10$, 12), are synthesized. Transition temperatures and phase characterization were studied by DSC, POM and XRD analyses. The dependence of phase transition temperatures on the terminal alkoxy chain lengths is discussed. With the increase in the terminal chain lengths, the thermal stability of the smectic mesophases of these liquid crystals was increased, and the smectic–isotropic transition temperatures in this series showed an even–odd effect.

Keywords: Bent-shaped liquid crystals; Dimers; Schiff base; Smectic; Even–odd effect

1. Introduction

Liquid crystalline dimers are attracting much attention because they exhibit variety of phases and serve as useful models for the semi-flexible, main-chain liquid crystal polymers [1–6]. In typical dimers where two individual mesogenic entities are attached to each other via flexible polymethylene spacer units, the structure of the mesophases can be modified through the change in spacer length and terminal chain length. The mesomorphic behaviour of an organic compound is basically dependent on its molecular architecture in which a slight change in the molecular geometry brings about considerable change in its mesomorphic properties. Most of these studies have been focused on Schiff's bases ever since the discovery of 4-methoxybenzylidene-4′-butylaniline (MBBA) which exhibits a room temperature nematic phase [7]. Over the past few decades, low molar mass Schiff's base esters have been investigated extensively. The introduction of a lateral polar hydroxyl group into the mesogenic fragment is known as an essential parameter leading to an increase in molecular polarizability as well as to an increase in the clearing temperature [8].

We have recently reported the synthesis and mesomorphic properties of dimeric ester Schiff bases (2ES-*n*) and azobenzenes (2A*n*) series in order to explore the thermal stability of liquid crystals and the relationship with its molecular structures. These two series of the bent-shaped dimers have a polar hydroxy group on the center of the short odd-numbered spacer, different terminal chains and mesogenic structure [9,10]. In the first series of 1,3-bis-(4-(4-alkyloxyphenyl-azo)phenoxy)propan-2-ols (2A*n*, $n = 4-10$, 12) with azobenzene mesogens, only smectic C mesophase was found in $n = 7-10$, 12, while the compounds ($n = 4-6$) with a short terminal chains were not liquid crystals [9].

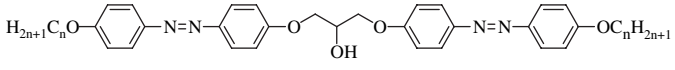

And in the second series, 1,3-bis-(4-(4-(4-alkyloxybenzoyloxy)benzylidene)aminophenoxy)-propan-2-ols (2ES-*n*, $n =$

* Corresponding author. Tel.: +82 42 629 7474; fax: +82 42 629 7469.
E-mail address: smlee@mail.hannam.ac.kr (S.-M. Lee).

0143-7208/$ - see front matter © 2006 Elsevier Ltd. All rights reserved.
doi:10.1016/j.dyepig.2006.07.015

5–10) with three benzene ring mesogenic structure, when the terminal chains ($n = 7$–10) are more than twice the spacer length, smectic A phase and nematic phase were found. While the compounds of $n = 5$–6 showed only the nematic phase, those ($n = 3$–4) with short terminal chains were not exhibiting any liquid crystalline phase [10].

In order to explore further the liquid crystallinity of bent-core dimers, and the relationship with its molecular structures, this article reports on the synthesis and the mesomorphic properties of symmetric Schiff base dimers ($2\mathbf{S}_n$), which have terminal alkoxy chains ($-OC_nH_{2n+1}$; $n = 5$–10, 12) and 2-hydroxy-1,3-dioxypropylene ($-OCH_2CH(OH)CH_2O-$) as a short odd-numbered spacer. The molecular structures of the title compounds were characterized by elemental analysis, Fourier transform infrared spectroscopy (FT-IR) and NMR techniques. Their liquid crystal properties were investigated by differential scanning calorimetry (DSC), polarizing optical microscopy (POM) and X-ray diffraction (XRD) measurements.

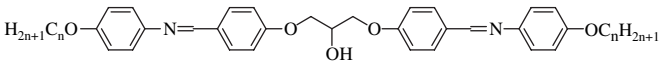

2. Experimental

2.1. Materials

1-Bromopentane, 1-bromohexane, 1-bromoheptane, 1-bromooctane, 1-bromononane, 1-bromodecane, 1-bromododecane, anhydrous EtOH, 4-nitrophenol, hydrazine monohydrate, 4-hydroxybenzaldehyde, NaOH, epichlorohydrin (ECH) and *p*-toluenesulfonic acid (PTSA) were GR grade reagents purchased from Aldrich Chemical Co. and used as received. All other solvents and reagents were purchased commercially and used without any further purification.

2.2. Synthesis

The synthetic route used in the preparation of Schiff base dimeric series involved four steps: (1) conventional etherification of 4-nitrophenol with an alkyl halide to produce the 4-alkoxynitrobenzenes, and then reduction of nitro group with hydrazine monohydrate to produce 4-alkoxyanilines (AB*n*); (2) reaction of 4-hydroxybenzaldehyde (2 eq.) with ECH (1 eq.) to produce 1,3-bis(4-formylphenoxy)-2-propanol (FPP-4); (3) condensation reactions of FPP-4 with 4-alkoxyanilines yield the diimine compounds. 1,3-Bis(4-formylphenoxy)propan-2-ol (FPP-4) was synthesized following the similar method described in the literature [11].

2.2.1. 1,3-Bis(4-((4-alkyloxyphenylimino)methyl)phenoxy)-propan-2-ol, $2\mathbf{S}_n$

The detailed synthetic procedures are as follows: FPP-4 (1 eq., 20 mmol) was dissolved in anhydrous EtOH (150 mL). 4-Alkyloxyaniline (2 eq., 40 mmol) and a catalytic quantity of PTSA were added into the solution, and then the mixture was stirred for 24 h at the room temperature. The resulting precipitate was isolated by filtration and purified by the recrystallization of both ethyl acetate/ethanol (1:1, v/v) and chloroform solvents. Final products were obtained as off-white crystals (72–98%). The data are listed below.

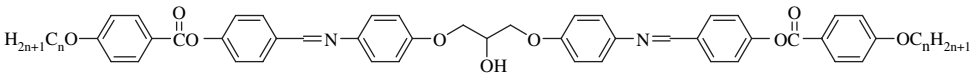

$2\mathbf{S}_5$: Yield, 91%. IR (KBr, cm^{-1}): 3472 (stretch., OH), 1604 (stretch., C=N). ^1H NMR (DMSO-d_6, ppm): δ 0.95 (t, 3H, $-CH_3$), 1.35 (m, 8H,$-(CH_2)_2-$), 1.74 (m, 2H, $-CH_2CH_2O-$), 4.01 (t, 2H, $-CH_2CH_2O-$), 4.16 (s, 2H, $-OCH_2CH(OH)-$), 4.28 (m, 1H, $-OCH_2CH(OH)-$), 6.91–7.92 (m, 8H, Ar–H), 8.62 (s, 1H, –CH=N). Elemental analysis: calcd for $C_{39}H_{46}N_2O_5$, C 75.21, H 7.44, N 4.50; found C 75.12, H 7.52, N 4.45%.

$2\mathbf{S}_6$: Yield, 72%. IR (KBr, cm^{-1}): 3470 (stretch., OH), 1625 (stretch., C=N), 1401, 1290 (stretch., C–O), 876 (stretch., C–N). Elemental analysis: calcd for $C_{41}H_{50}N_2O_5$, C 75.66, H 7.74, N 4.30; found C 75.60, H 7.80, N 4.41%. ^1H NMR (DMSO-d_6, ppm): δ 0.95 (t, 3H, $-CH_3$), 1.35 (m, 8H, $-(CH_2)_2-$), 1.74 (m, 2H, $-CH_2CH_2O-$), 4.01 (t, 2H, $-CH_2CH_2O-$), 4.16 (s, 2H, $-OCH_2CH(OH)-$), 4.28 (m, 1H, $-OCH_2CH(OH)-$), 6.91–7.92 (m, 8H, Ar–H), 8.62 (s, 1H, –CH=N).

$2\mathbf{S}_7$: Yield, 94%. IR (KBr, cm^{-1}): 3468 (stretch., OH), 1602 (stretch., C=N). ^1H NMR (DMSO-d_6, ppm): δ 0.95 (t, 3H, $-CH_3$), 1.34 (m, 8H, $-(CH_2)_4-$), 1.76 (m, 2H, $-CH_2CH_2O-$), 4.01 (t, 2H, $-CH_2CH_2O-$), 6.91–7.91 (m, 8H, Ar–H), 4.19 (s, 2H, $-OCH_2CH(OH)-$), 4.25 (m, 1H, $-OCH_2CH(OH)-$), 8.61 (s, 1H, –CH=N). Elemental analysis: calcd for $C_{43}H_{54}N_2O_5$, C 76.07, H 8.02, N 4.13; found C 75.98, H 8.09, N 4.15%.

$2\mathbf{S}_8$: Yield, 74%. IR (KBr, cm^{-1}): 3466 (stretch., OH), 1621 (stretch., C=N), 1407, 1289 (stretch., C–O), 880 (stretch., C–N). Elemental analysis: calcd for $C_{45}H_{58}N_2O_5$, C 76.45, H 8.27, N 3.96; found C 76.51, H 8.30, N 4.01%. ^1H NMR (DMSO-d_6, ppm): δ 0.95 (t, 3H, $-CH_3$), 1.35 (m, 8H,$-(CH_2)_2-$), 1.74 (m, 2H, $-CH_2CH_2O-$), 4.01 (t, 2H, $-CH_2CH_2O-$), 4.16 (s, 2H, $-OCH_2CH(OH)-$), 4.28 (m, 1H, $-OCH_2CH(OH)-$), 6.91–7.92 (m, 8H, Ar–H), 8.62 (s, 1H, –CH=N).

$2\mathbf{S}_9$: Yield, 98%. IR (KBr, cm^{-1}): 3474 (stretch., OH), 1604 (stretch., C=N). ^1H NMR (DMSO-d_6, ppm): δ 0.94 (t, 3H, $-CH_3$), 1.38 (m, 8H, $-(CH_2)_4-$), 1.76 (m, 2H, $-CH_2CH_2O-$), 4.01 (t, 2H, $-CH_2CH_2O-$), 4.18 (s, 2H, $-OCH_2CH(OH)-$), 4.24 (m, 1H, $-OCH_2CH(OH)-$), 6.91–7.92 (m, 8H, Ar–H),

8.64 (s, 1H, −C═N). Elemental analysis: calcd for $C_{47}H_{62}N_2O_5$, C 76.80, H 8.50, N 3.81; found C 76.79, H 8.55, N 3.85%.

$2\mathbf{S}_{10}$: Yield, 85%. IR (KBr, cm^{-1}): 3470 (stretch., OH), 1620 (stretch., C═N), 1401, 1292 (stretch., C−O), 875 (stretch., C−N). Elemental analysis: calcd for $C_{49}H_{66}N_2O_5$, C 77.13, H 8.72, N 3.67; found C 77.09, H 8.69, N 3.72%. ^{1}H NMR (DMSO-d_6, ppm): δ 0.95 (t, 3H, $-CH_3$), 1.35 (m, 8H, $-(CH_2)_2-$), 1.74 (m, 2H, $-CH_2CH_2O-$), 4.01 (t, 2H, $-CH_2CH_2O-$), 4.16 (s, 2H, $-OCH_2CH(OH)-$), 4.28 (m, 1H, $-OCH_2CH(OH)-$), 6.91−7.92 (m, 8H, Ar−H), 8.62 (s, 1H, −CH═N).

$2\mathbf{S}_{12}$: Yield, 80%. IR (KBr, cm^{-1}): 3471 (stretch., OH), 1619 (stretch., C═N), 1401, 1292 (stretch., C−O), 875 (stretch., C−N). Elemental analysis: calcd for $C_{53}H_{74}N_2O_5$, C 77.71, H 9.11, N 3.42; found C 77.75, H 9.08, N 3.29%. ^{1}H NMR (DMSO-d_6, ppm): δ 0.95 (t, 3H, $-CH_3$), 1.35 (m, 8H,$-(CH_2)_2-$), 1.74 (m, 2H, $-CH_2CH_2O-$), 4.01 (t, 2H, $-CH_2CH_2O-$), 4.16 (s, 2H, $-OCH_2CH(OH)-$), 4.28 (m, 1H, $-OCH_2CH(OH)-$), 6.91−7.92 (m, 8H, Ar−H), 8.62 (s, 1H, −CH═N).

2.3. Measurements

IR spectra were obtained by a Perkin−Elmer model 1000 FT-IR spectrophotometer on KBr pellet. ^{1}H NMR spectra were recorded by using a Varian Gemini 300 NMR spectrometer at 23 or 80 °C. Elemental analysis was performed by Flash EA 1112 Series (CE instruments). Differential scanning calorimetric measurements were performed using a TA instruments 910S DSC apparatus under dry nitrogen flow (5 °C/min). The transition temperatures were taken at the maximum point of the peaks for each sample. The transition enthalpies were evaluated from the integrated area of the endothermic peaks using a reference indium sample as the standard. Optical micrographs were obtained by using a Nikon Labophot-2 polarizing microscope fitted with an RTC-1 temperature controller (Instec Inc., Broomfield, Co.) and a Mettler FP-82HT hot stage (−2 °C/min, ×100). Small and wide angle X-ray scatterings (SAXS and WAXS) were performed at the X-ray beam line (3C2 and 4C2) in Pohang Accelerator Laboratory, S. Korea.

3. Results and discussion

These new bent-shaped dimers, 1,3-bis(4-((4-alkyloxyphenylimino)methyl)phenoxy)propan-2-ols ($2\mathbf{S}_n$; $n = 5-10$, 12), were synthesized starting from dialdehyde derivative (FPP-4). The dimesogens, $2\mathbf{S}_n$, were then obtained by the condensation reaction between amines and dialdehyde (see Scheme 1).

The mesomorphic properties of the dimers were determined by means of DSC, POM and XRD. The thermal transition temperatures and thermodynamic parameters for dimers are summarized in Table 1. Subsequent increases in the length of the terminal chains cause the clearing temperatures to fall, showing initially an alternation which attenuates with increasing n. As n increases the smectic phase stability increases as would be anticipated. Thus the effects on the transition temperatures and phase behaviour of increasing the length of terminal chains in symmetric bent-shaped liquid crystal dimers are in

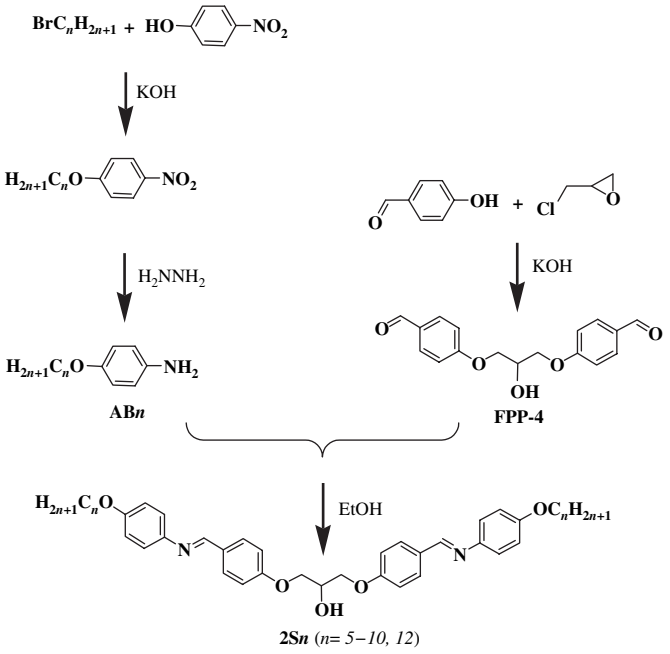

Scheme 1. Synthetic pathways for dimers ($2\mathbf{S}_n$).

accord with those observed for conventional low molar mass mesogens. For compounds of $n = 6-9$, enantiotropic smectic A phase was emerged, while for those of $n = 10$ and 12 with long terminal chains, enantiotropic smectic A phase and smectic C phase were formed.

Representative DSC traces for dimers are presented in Fig. 1. In heating and cooling scans of the odd-numbered member ($2\mathbf{S}_9$), it shows K to smectic A phase transition at 168.2 °C and smectic A to isotropic phase transition at 190.8 °C. Smectic A−K transition temperature shows the most supercooling during the cooling scan when compared to other phase transition temperatures. In both scans of the even-numbered member ($2\mathbf{S}_{10}$), it shows K to smectic C phase transition at 166.7 °C, smectic C to smectic A transition at 183.9 °C and smectic A to isotropic phase transition at 194.6 °C. Fig. 2(a) shows bâtonnets developing to focal conic fan textures at the clearing point of $2\mathbf{S}_8$ (192 °C). Fig. 2(b) shows the typical smectic A phase texture (focal conic fan textures) exhibited by $2\mathbf{S}_9$. Optical textures

Table 1
Thermal transition behaviors and thermodynamic data for the phase transition of $2\mathbf{S}_n$ series

n	Phases and transition temperatures (°C) (ΔH, kJ/mol)[a]
12	K 153.8 (116.6), SmC 183.7 (−)[b], SmA 190.7 (14.7) I
10	K 157.5 (74.6), SmC 182.1 (−)[b], SmA 193.0 (18.8) I
9	K 157.8 (54.6), SmA 185.9 (12.7) I
8	K 166.1 (36.8), SmA 193.7 (6.38) I
7	K 166.8 (35.8), SmA 180.4 (4.08) I
6	K 178.0 (35.9), SmA 189.4 (7.46) I
5	K 182.2 (64.4) I

[a] K = crystalline state, SmC = smectic C, SmA = smectic A, I = isotropic state, all data were obtained from second cooling scan at −5 °C/min.

[b] Enthalpy is very small and the transition temperature has been determined by optical microscopic observation.

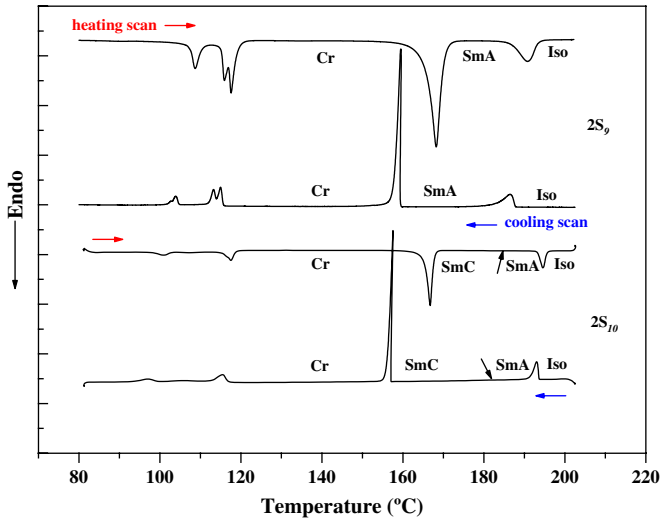

Fig. 1. Differential scanning calorimetry curves for dimers ($2\mathbf{S}_9$, $2\mathbf{S}_{10}$) in the heating and cooling scans (5 °C/min). The arrows indicate that the temperatures at the SmA–SmC transition are observed in optical microscopy.

of $2\mathbf{S}_{10}$ (Fig. 2(c) and (d)) reveal that a homeotropic with spherulitic domains and fan texture for smectic A phase (190 °C) transforms into a schlieren and broken fan-shaped texture for smectic C phase (178 °C) on cooling. Similar results have been reported by Weissflog et al. [12].

The temperature-dependent X-ray diffraction patterns obtained from powder samples of $2\mathbf{S}_{10}$ at 185.1 and 175.0 °C are presented in Fig. 3. A broad halo at wide angles (associated with the lateral packings: inset) and a sharp reflection at low angles (associated with the smectic layers) are shown in both patterns (Fig. 3(a) and (b)). The scattered intensity curve (a)

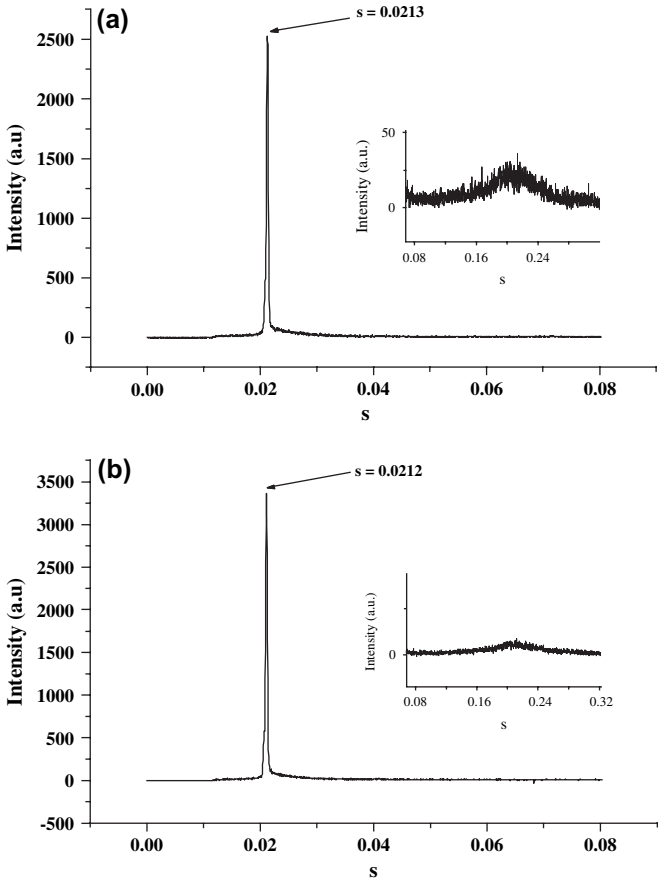

Fig. 3. The intensity profile of the small-angle X-ray diffraction pattern at (a) SmA phase (185.1 °C) and (b) SmC phase (175.0 °C) of $2\mathbf{S}_{10}$. (Scattering vector, s (Å) $= 2 \sin\theta/\lambda = 1/d$, $q = 2\pi/d$.)

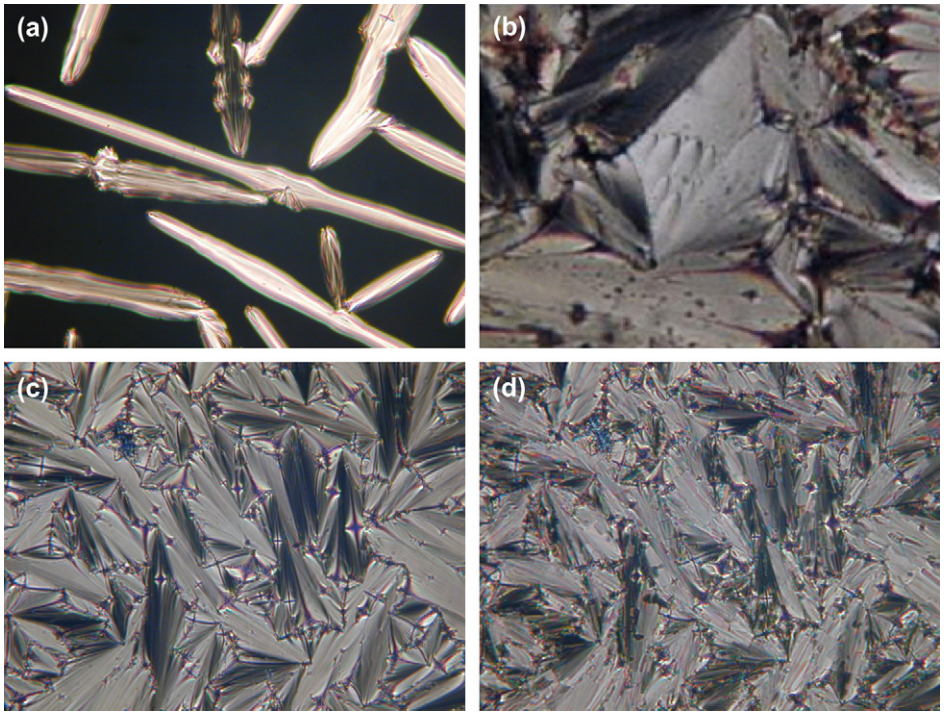

Fig. 2. Optical textures of (a) bâtonnets of $2\mathbf{S}_8$ (192 °C); (b) SmA, focal conic fan texture of $2\mathbf{S}_9$ (171 °C); (c) SmA, the fan texture with spherulitic domains on homeotropic areas ($2\mathbf{S}_{10}$, 190 °C); (d) SmC, the *schlieren* and broken-fan shaped textures ($2\mathbf{S}_{10}$, 178 °C).

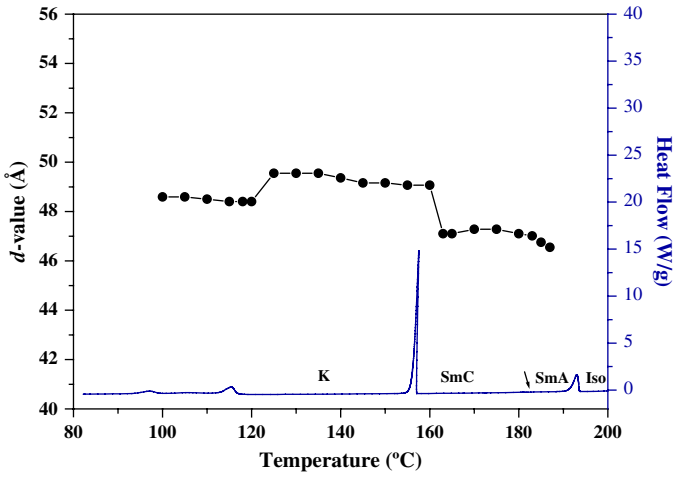

Fig. 4. The temperature dependence of the layer spacing in the crystal states, SmC and SmA phases of $2\mathbf{S}_{10}$.

obtained at 185.1 °C reveals a diffuse halo centered at about 4.65 Å and a sharp first-order reflection at $d = 47.0$ Å (molecular length obtained by modeling is $l = 49.89$ Å). The intensity curve (b) at 175.0 °C also discloses a very similar pattern ($d = 47.2$ Å). In Fig. 4, the temperature dependence of the layer spacing in all phases exhibited by $2\mathbf{S}_{10}$ is depicted. The temperature dependence of the layer spacing of the smectic C and A phases is consistent with the thermal and optical transitions observed by the differential scanning calorimetry and optical microscopy. On decreasing the temperature, the layer spacing measured in the smectic A phase increases and this reflects, in portion, an inhibition of the molecular orientational fluctuations and an increase in the conformational order. At the transition to the smectic C phase, the layer spacing decreases and this continues throughout the temperature range of the phase. This results from the tilting of the director of bent molecules with respect to the layer normal and subsequent growth of the tilt angle with the temperature decrease.

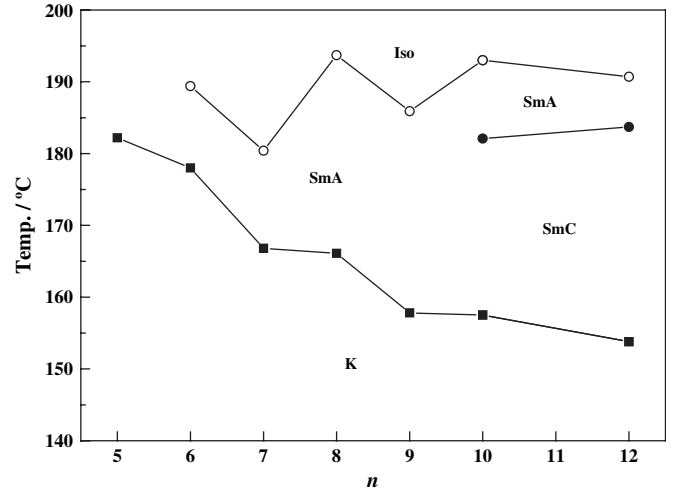

Fig. 5. The dependence of the transition temperatures on the number of carbon atoms, n, in the terminal alkoxy chains for the $2\mathbf{S}_n$ series. The Iso–SmA transition is indicated by ○, SmA–SmC transition by ● and SmA/SmC/Iso–K transition by ■.

The dependence of the phase transition temperatures on terminal chain length is plotted in Fig. 5. The clearing temperatures appear to show an even–odd alternation effect as a function of the parity of the terminal chains. The clearing enthalpies and entropies show such effect only for the early members ($n = 6$–8) of the series. The result seems to demonstrate that the tendency toward smectic mesomorphism increases with increasing terminal alkoxy chain length. And on increasing the length of the terminal alkoxy chains for this series, the thermal stability of tilted smectic phase increases. This may be the result of the terminal alkoxy chains lying at an angle to the long molecular axis inducing the molecular tilt between neighboring molecules.

4. Conclusion

New series ($2\mathbf{S}_n$) of symmetric liquid crystal dimers, where two Schiff base mesogenic units are connected by a 2-hydroxy-1,3-dioxypropylene spacer, have been prepared. All dimers showed the smectic mesomorphism except for $2\mathbf{S}_5$. Schiff base mesogenic dimers with long chains ($2\mathbf{S}_{10}$, $2\mathbf{S}_{12}$) presented smectic C and smectic A phases, while intermediate terminal chains ($2\mathbf{S}_6$–$2\mathbf{S}_9$) showed smectic A phase. However, $2\mathbf{S}_5$ compound with short chains was not exhibiting any liquid crystalline phase. Our results suggested that the dimers with the Schiff base mesogens ($2\mathbf{S}_n$) could be more conducive to smectic mesomorphism when compared with those of the azobenzene analogous (2An) [9].

Acknowledgements

X-ray diffraction measurements were performed at the 3C2 and 4C1 beamline in Pohang Accelerator Laboratory, Korea.

References

[1] Imrie CT, Henderson PA. Curr Opin Colloid Interface Sci 2002;7:298.
[2] Weissflog W, Lischka CH, Diele S, Wirth I, Pelzl G. Liq Cryst 2000;27:43.
[3] Prasad V, Lee K-H, Park YS, Lee J-W, Oh D-K, Han DY, et al. Liq Cryst 2002;29:1113.
[4] Takanishi Y, Izumi T, Watanabe J, Ishikawa K, Takezoe H, Iida A. J Mater Chem 1999;9:2771.
[5] Choi E-J, Choi B-K, Kim J-H, Jin J-I. Bull Korean Chem Soc 2000;21:110.
[6] Ganicz T, Stanczyk WA, Białecka-Florjańczyk E, Śledzińska I. Polymer 1999;40:4733.
[7] Kelker H, Scheurle B. Angew Chem Int Ed 1969;81:903.
[8] Yeap GY, Ha ST, Lim PL, Boey PL, Mahmood WAK, Ito MM, et al. Mol Cryst liq Cryst 2004;423:73.
[9] (a) So B-K, Jang M-C, Park J-H, Lee K-S, Song HH, Lee S-M. Opt Mater 2003;21:685. reference there in;
(b) So B-K, Kim W-J, Lee S-M, Song HH, Park J-H. Dyes Pigments 2006;70:38.
[10] So B-K, Kim Y-S, Choi M-M, Lee S-M, Kim J-E, Song HH, et al. Liq Cryst 2004;31:169.
[11] Zhao B, Wu YJ, Tao JC, Yuan HZ, Mao XA. Polyhedron 1996;15:1197.
[12] Weissflog W, Kovalenko L, Wirth I, Diele S, Pelzl G, Schmalfuss H, et al. Liq Cryst 2000;27:677.